Psychopharmacology
DOI 10.1007/s00213-011-2603-y

ORIGINAL INVESTIGATION

Characterizing the effects of Eugenol on neuronal ionic currents and hyperexcitability

Chin-Wei Huang · Julie Chi Chow · Jing-Jane Tsai · Sheng-Nan Wu

Received: 27 June 2011 / Accepted: 26 November 2011

Abstract
Rationale Eugenol (EUG, 4-allyl-2-methoxyphenol), the main component of essential oil extracted from cloves, has various uses in medicine because of its potential to modulate neuronal excitability. However, its effects on the ionic mechanisms remains incompletely understood.
Objectives We aimed to investigate EUG's effects on neuronal ionic currents and excitability, especially on voltage-gated ion currents, and to verify the effects on a hyperexcitability-temporal lobe seizure model.
Methods With the aid of patch-clamp technology, we first investigated the effects of EUG on ionic currents in NG108-15 neuronal cells differentiated with cyclic AMP. We then used modified Pinsky–Rinzel simulation modeling to evaluate its effects on spontaneous action potentials (APs). Finally, we investigated its effects on pilocarpine-induced seizures in rats.
Results EUG depressed the transient and late components of I_{Na} in the neurons. It not only increased the degree of I_{Na} inactivation, but specifically suppressed the non-inactivating I_{Na} ($I_{Na(NI)}$). Its inhibition of $I_{Na(NI)}$ was reversed by tefluthrin. In addition, EUG diminished L-type Ca^{2+} current and delayed rectifier K^+ current only at higher concentrations. EUG's effects on APs frequency reduction was verified by the simulation modeling. In pilocarpine-induced seizures, the EUG-treated rats showed no shorter seizure latency but a lower seizure severity and mortality than the control rats. The EUG's effect on seizure severity was occluded by the $I_{Na(NI)}$ antagonist riluzole.
Conclusion The synergistic blocking effects of I_{Na} and $I_{Na(NI)}$ contributes to the main mechanism through which EUG affects the firing of neuronal APs and modulate neuronal hyperexcitability such as pilocarpine-induced temporal lobe seizures.

Keywords Eugenol · Na^+ current · Ca^{2+} current · K^+ current · Action potential · Neuron

C.-W. Huang · J.-J. Tsai
Department of Neurology,
National Cheng Kung University Hospital,
Tainan, Taiwan

J. C. Chow
Department of Pediatric Neurology,
Chi-Mei Foundation Medical Center,
Tainan, Taiwan

S.-N. Wu
Department of Physiology,
National Cheng Kung University Medical College,
1 University Road,
Tainan 70101, Taiwan

S.-N. Wu (✉)
Institute of Basic Medical Sciences,
National Cheng Kung University Medical College,
Tainan, Taiwan
e-mail: snwu@mail.ncku.edu.tw

Introduction

Eugenol (EUG, 4-allyl-2-methoxyphenol), an aromatic molecule found in plants including clove, bay leaves and allspice, has been used in medicine to relieve pain arising from a variety of sources, such as pulpal inflammation and dentin hypersensitivity (Bender 2000; Köseoğlu et al. 2006). In the central nervous system, EUG is neuroprotective against excitotoxicity, cerebral ischemia, and the toxic effects of

Published online: 13 December 2011

amyloid-β peptides (Won et al. 1998; Irie and Keung 2003). It has been reported to protect animals against generalized seizure models induced by maximal electroshock or pentylenetetrazole (Dallmeier et al. 1983; Pourgholami et al. 1999; Freire et al. 2006).

For EUG-induced local analgesia, it might inhibit transient voltage-gated Na^+ currents (I_{Na}) in rat dental primary afferent neurons (Park et al. 2009) and rat dorsal root ganglion neurons (Cho et al. 2008). Additionally, EUG could suppress epileptiform field potentials and spreading depression in hippocampus and neocortex in vitro (Müller et al. 2006). Although inhibiting transient I_{Na} suppresses impulse generation and propagation in some neurons, why EUG could attenuate a complex epileptic network activity is still not completely understood. Whether EUG has the protective effects against hyperexcitability disorders such as partial epilepsy remains unknown.

The non-inactivating Na^+ currents ($I_{Na(NI)}$) might be a potential target for EUG. $I_{Na(NI)}$, which is important in regulating the firing properties of neuronal action potentials (AP), is responsible for the generation of network epileptiform activity (Segal and Douglas 1997; Stafstrom 2007). Recent studies demonstrated that pilocarpine-induced epileptic seizures, a standard animal model of temporal lobe seizures, induce a significant increase in $I_{Na(NI)}$ which is important in intrinsic bursting behaviors in the epileptic network, contributing to epileptogenesis (Chen et al. 2011). Whether EUG has important effects on $I_{Na(NI)}$ and how does EUG synergistically affect I_{Na} and $I_{Na(NI)}$ remain to be investigated.

We recently characterized an $I_{Na(NI)}$ in NG108-15 cells (a somatic cell hybrid; mouse neuroblastoma and rat gliomas cells) differentiated with an analogue of cyclic adenosine monophosphate (Huang et al. 2008; Wu et al. 2009a). This neuronal cell line has been widely used as a neuron model in electrophysiology and pharmacology researches (Meves et al. 1999; Wu et al. 2001; Tsai et al. 2006). In these cells after differentiation, $Na_V1.7$, as a voltage-gated sodium channel with a critical role in the generation and conduction of actional potentials, showed significantly higher expression levels (Kawaguchi et al. 2007).

In addition to I_{Na}, previous studies demonstrated the ability of EUG to bind to vanilloid receptors and, in turn, to activate non-selective cation channels (Ohkubo and Kitamura 1997; Yang et al. 2003). EUG inhibited voltage-gated Ca^{2+} (Ca_v) current through $Ca_V2.3$ channels in the E52 cell line (Chung et al. 2008), which is thought to be direct and independent of its binding to vanilloid receptors or β-adrenergic receptors (Wu et al. 2000; Yang et al. 2003). The important regulators of neuronal excitability include the L-type Ca^{2+} current ($I_{Ca,L}$) which allow large calcium influx, activating downstream pathway involving synaptic plasticity in hippocampus and cortex (Benarroch 2010; Earl and Tietz 2011), and the delayed-rectifier K^+ currents ($I_{K(DR)}$) which play a major role in the control of resting membrane potential and spike frequency adaptation (Coetzee et al. 1999; He et al. 2010; Huang et al. 2011). Whether EUG has effects on these channels is unknown.

We therefore aimed to determine whether EUG has specific effect on ionic currents (I_{Na}, $I_{Na(NI)}$, $I_{Ca,L}$, and $I_{K(DR)}$), firing behaviors in neurons and pilocarpine-induced temporal lobe seizures.

Materials and methods

Cell preparations

The mouse neuroblastoma×rat glioma hybrid cell line (NG108-15) was obtained from the European Collection of Cell Cultures (ECACC-88112302; Wiltshire, UK). Cells were grown in monolayer cultures at a density of 10^6/ml in plastic disks containing Dulbecco's modified Eagle's medium supplemented with 100 μM hypoxanthine, 1 μM aminopterin, 16 μM thymidine, and 5% fetal bovine serum, in a humidified environment of 5% CO_2/95% air at 37°C. To induce neuronal differentiation, the culture medium was replaced with a medium containing 1 mM dibutyryl cAMP, and the cells were maintained in an incubator for another 1–7 days (Lin et al. 2008; Chen et al. 2009). To observe neurite growth, a Nikon Eclipse Ti-E inverted microscope (Li Trading Co., Taipei, Taiwan) equipped with a 5-megapixel cooled digital camera was used. The digital camera was connected to a personal computer controlled by NIS-Elements BR3.0 software (Nikon, Kanagawa, Japan). The number of neurites and varicosities was increased when cells were pre-incubated with 1 mM dibutyryl cAMP. Cell viability was evaluated using a WST-1 assay (Roche-Diagnostics, Indianapolis, IN) and an ELISA reader (Dynatech, Chantilly, VA, USA).

Electrophysiological measurements

Cells were dissociated with 1% trypsin/EDTA solution, and an aliquot of cell suspension was transferred to a recording chamber affixed to the stage of a DM-IL inverted microscope (Leica, Wetzlar, Germany). Cells were bathed at room temperature (20–25°C) in normal Tyrode's solution containing 1.8 mM $CaCl_2$. The electrodes were pulled from Kmax-51 capillaries (Kimble Glass, Vineland, NJ) in a PP-830 puller (Narishige, Tokyo), and these, which had a resistance of 3–5 MΩ when filled with different intracellular solutions, were subsequently mounted on and controlled by a WR-98 hydraulic micromanipulator (Narishige, Tokyo, Japan). The

whole-cell configuration of a patch-clamp technique was carried out using an RK-400 amplifier (Bio-Logic, Claix, France) or an Axopatch-200B amplifier (Molecular Devices, Sunnyvale, CA, USA; Lin et al. 2004; Huang et al. 2010). EUG was dissolved in DMSO (less than 0.01%) and made immediately prior to experiments. Tested drugs were applied by perfusion or added to the bath to obtain the final concentrations indicated. Vehicle control experiments were done and no definite effects on sodium currents were observed, supported by a previous study (Ohkubo and Kitamura 1997).

The signals were displayed on an HM-507 oscilloscope (Hameg, East Meadow, NY, USA) and a liquid crystal projector (AV600; Delta, Taipei, Taiwan). The data were stored online in a TravelMate-6253 laptop computer (Acer, Taipei, Taiwan) at 10 kHz through a Digidata-1322A interface (Molecular Devices). The latter device was equipped with an Adaptec SlimSCSI card (Milpitas, CA, USA) via a PCMCIA slot, and controlled by pCLAMP 9.2 (Molecular Devices). Current signals were low-pass filtered at 1 or 3 KHz. The signals were analyzed using pCLAMP 9.2 (Molecular Devices) or Origin 7.5 (OriginLab, Northampton, MA, USA). The pCLAMP-generated voltage-step protocols were used to examine the current–voltage (*I-V*) relationships for ion currents (e.g. I_{Na} and $I_{K(DR)}$).

Simulation modeling

Spontaneous discharge of NG108-15 neurons was simulated with the aid of the Pinsky-Rinzel model (Pinsky and Rinzel 1994) and modified by Huang et al (Huang et al. 2008). Some of default parameters used in this study were modified and shown in Table 1.

Table 1 Default parameters used for the modeling of NG108-15 neurons in this study

Symbol	Description	Value
C_m	Membrane capacitance	3 μF
g_{Na}	Na^+ current conductance	18 nS
$g_{Na(ni)}$	Non-inactivating Na^+ current conductance	0.5 nS
$g_{K(DR)}$	Delayed rectifier K^+ current conductance	24 nS
g_{Ca}	Ca^{2+} current conductance	1 nS
$g_{K(AHP)}$	After-hyperpolarization K^+ current conductance	2.5 nS
$g_{K(Ca)}$	Ca^{2+}-activated K^+ current conductance	20 nS
$g_{K(ATP)}$	ATP-sensitive K^+ current conductance	0.3 nS
V_{Na}	Na^+ reversal potential	+60 mV
V_{Ca}	Ca^{2+} reversal potential	+80 mV
V_K	K^+ reversal potential	−75 mV

The $I_{Na(NI)}$ used in this study had no inactivation and was determined as follows:

$$I_{Na\,(NI)} = g_{Na(NI)} \times (V - V_{Na}),$$

$$g_{Na\,(NI)} = g_{Na(NI)\,\max} \times m_{Na\,(NI)},$$

$$\frac{dm_{Na\,(NI)}}{dt} = \frac{m_{\infty Na\,(NI)} - m_{Na\,(NI)}}{\tau_{mNa(NI)}},$$

$$m_{\infty Na\,(NI)} = \frac{1}{1 + \exp(-(V - 27)/7)},$$

$$\tau_{mNa\,(NI)} = \frac{1}{\alpha_{m(Na)} + \beta_{m(Na)}}$$

where $m_{\infty Na(NI)}$ represents the steady state of activation variable of $I_{Na(NI)}$. The parameter value of $m_{\infty Na(NI)}$ was originally taken from the paper of Wu et al. (2009a). $\alpha_{m(Na)}$ and $\beta_{m(Na)}$ are the forward and backward rate constants of activation variable (m) for I_{Na}, respectively.

Simulations were undertaken in C++ programming language or within the simulation package XPPAUT on a Hewlett Packard Workstation (HPxw9300; Palo Alto, CA). Source files used in this study can be available from http://www.math.pitt.edu/~bard/XPP/XPP.html. Several different integration algorithms (e.g. backward Euler and Cvode) and time steps were used to check accuracy and stability.

Pilocarpine-induced epileptic seizures

All experiments were conducted in accordance with the specifications of the ethical committee of National Cheng Kung University. Procedures for animal experimentation were reviewed and approved by the Institutional Animal Care and Use Committee. The procedures used were as humane as possible. Adult Sprague–Dawley (SD) male rats weighing 175–200 g were purchased from National Cheng Kung University, being housed under a 12 h light–dark cycle with food and water ad libitum. They were divided into five groups: one (control group) with normal saline injection (i.p.); three (EUG, eugenolol and eugenodilol group) were given 100 mg/kg of each drug (i.p.) 30 min before the seizure induction (Sayyah et al. 2002). For evaluation of the EUG's *in vivo* effect on the $I_{Na(NI)}$, the $I_{Na(NI)}$ antagonist, riluzole was injected (8 mg/kg, i.p.) 30 min before the injection of EUG (RLZ+EUG group). For seizure induction, they were all given a lithium chloride (Sigma–Aldrich Co., St Louis, MO) injection (3 meq/kg, i.p.) 18–20 h before a subcutaneous (s.c.) pilocarpine injection (60 mg/kg; Sigma-Aldrich) to induce SE, and, to reduce the peripheral consequences of pilocarpine, methylscopolamine injection (25 mg/kg, s.c.; Sigma-Aldrich) 30 min before the pilocarpine injection (Huang et al. 2009; Duarte et al. 2010). The stages of seizure were determined based on

the standard criteria (Racine et al. 1973; Pitkanen et al. 2006; Cifelli and Grace 2011). Typically, within 5 min of the pilocarpine injection, the rats developed piloerection and other signs of cholinergic stimulation. Over the following 15 to 20 min, they exhibited mouth and facial movements, head bobbing and nodding, scratching, masticatory automatisms, and exploratory behavior (stages 1–2). Episodes of head and bilateral forelimb myoclonic movements (stage 3) started at around 20 to 25 min and progressed to status epilepticus (stages 4–5) with rearing and falling at about 50 min after the pilocarpine injection. All these seizure experiments were done by two independent observers who were blind to the experimental design.

For all the rats, the time intervals to the onset of seizure behaviors, the seizure severity and mortality were compared among the control, the EUG, the RLZ+EUG group, the eugenolol and the eugenodilol group, and. The seizure-related mortality was calculated during the first 24 h after status epilepticus.

Data analyses

To calculate percentage inhibition of EUG on $I_{Na,}$ the current amplitudes during the application of EUG were compared with those measured after a subsequent application of 1 μM tetrodotoxin (TTX). The concentration-dependent relations of EUG on the inhibition of I_{Na} measured at the beginning and end of depolarizing pulses from −80 to −10 mV were fitted to the Hill equation. That is, Percentage inhibition $= (E_{max} \times [drug]^n)/(IC_{50}{}^n + [drug]^n)$, where [drug] represents the EUG concentration; IC_{50} and n are the half-maximal inhibitory concentration and the Hill coefficient, respectively; and E_{max} is the EUG-induced maximal inhibition of I_{Na} (i.e. TTX-sensitive current).

The inhibitory effects of EUG on I_{Na} can be explained by a state-dependent blocker that binds to the open state of the channel according to a minimal kinetic scheme (Wu et al. 2009b):

$$C \underset{\beta}{\overset{a}{\rightleftarrows}} O \underset{k_{-1}}{\overset{k_{+1}}{\rightleftarrows}} O \cdot B,$$

where α and β are the voltage-dependent rate constants for the opening and closing of the Na_V channel; k_{+1} and k_{-1} are those for blocking and unblocking by EUG (i.e. the on- and off-rate constants for EUG) and [B] is the blocker (i.e. EUG) concentration. C, O and O·B are the closed, open and open-blocked states, respectively.

The blocking and unblocking rate constants, k_{+1} and k_{-1}, were determined from the slow component of inactivation time constants ($\tau_{inact(S)}$) for I_{Na} evoked by the depolarizing pulses. Blocking and unblocking rate constants were estimated using the relation: $1/\tau_b = k_{+1} \times [B] + k_{-1}$, where k_{+1} and k_{-1}, respectively, result from the slope and the y-axis intercept at [B]=0 of the linear regression interpolating the reciprocal time constants (i.e. $1/\tau_b$) versus different EUG concentrations.

For acute seizure study, the latency to the first seizure was analyzed by non-repeated measures analysis of variance. The percentage of severe seizures and mortality among the three groups were analyzed and compared by Yates' correction for continuity test. For in vitro study, all values were given as means±SEM with sample sizes (n) indicating the number of cells examined. The paired or unpaired Student's t test and one-way ANOVA were used for the statistical evaluation of difference among means. Statistical analyses were performed using SPSS 14.0 (SPSS Inc., Chicago, IL, USA). A difference with a p value<0.05 was considered statistically significant.

Drugs and solutions

EUG, tefluthrin, riluzole, tetrandrine, tetraethylammonium chloride (TEA) were obtained from Sigma–Aldrich (St. Louis, MO, USA), and tetrodotoxin (TTX) was from Alomone Labs (Jerusalem, Israel), and dibutyryl cAMP and tetrandrine were from Biomol (Plymouth Meeting, PA, USA). Salmeterol was from Tocris (Bristol, UK). Eugenolol and Eugenodilol were gifts from Dr. Jwu-Lai Yeh, Department of Pharmacology, Kaohsiung Medical University, Kaohsiung City, Taiwan (Chen et al. 1997; Huang et al. 1999; Wu et al. 2000). EUG, salmeterol and tefluthrin were dissolved in dimethylsulfoxide to make a stock solution and kept at −20°C. Eugenolol and eugenodilol were solubilized in 10% absolute alcohol and then diluted with distilled water.

The composition of normal Tyrode's solution was as follows (in mM): NaCl 136.5, KCl 5.4, $CaCl_2$ 1.8, $MgCl_2$ 0.53, glucose 5.5, and HEPES-NaOH buffer 5.5 (pH 7.4). To record membrane potential or $I_{K(DR)}$, the patch pipette was filled with a solution (in mM): KCl 140, $MgCl_2$ 1, Na_2ATP 3, Na_2GTP 0.1, EGTA 0.1, and HEPES-KOH buffer 5 (pH 7.2). To measure I_{Na} or $I_{Ca,L}$, K^+ ions inside the pipette solution were replaced with equimolar Cs^+ ions, and the pH was adjusted to 7.2 with CsOH.

Results

Inhibitory effect of EUG on I_{Na} in differentiated NG108-15 neuronal cells

In the initial set of experiments, a whole-cell configuration was used to investigate the effect of EUG on macroscopic ion currents in NG108-15 cells. The cells were bathed in Ca^{2+}-free Tyrode's solution containing 10 mM of TEA and

patch pipettes were loaded with a Cs^+-containing solution. When the depolarizing pulses from −80 mV to different membrane potentials were applied to evoke I_{Na}, applying EUG diminished the peak amplitude of I_{Na}, together with a progressive increase in current decay (Fig. 1a). For example, when cells were depolarized from −80 to −10 mV, cell exposure to EUG (10 μM) caused a significant reduction in the peak amplitude of I_{Na} from 5145±855 to 2985±654 pA (n=8). The time constants in the slow component of current inactivation (i.e. $\tau_{inact(S)}$) was significantly decreased to 4.8±0.1 ms from a control value of 10.2±0.2 ms (n=7). Similarly, the deactivation rate of I_{Na} was progressively increased in the presence of EUG. However, no discernible change in the overall *I-V* relationship of I_{Na} can be demonstrated in the presence of 10 μM EUG (Fig. 1b).

It is also notable that the magnitude of EUG-mediated inhibition of I_{Na} measured at the beginning and end of the depolarizing pulses was found to be different. EUG concentration-dependently suppressed the transient and late components of I_{Na}. The relationships between the EUG concentration and the percentage inhibition for transient and late components of I_{Na} are illustrated in Fig. 1c. The

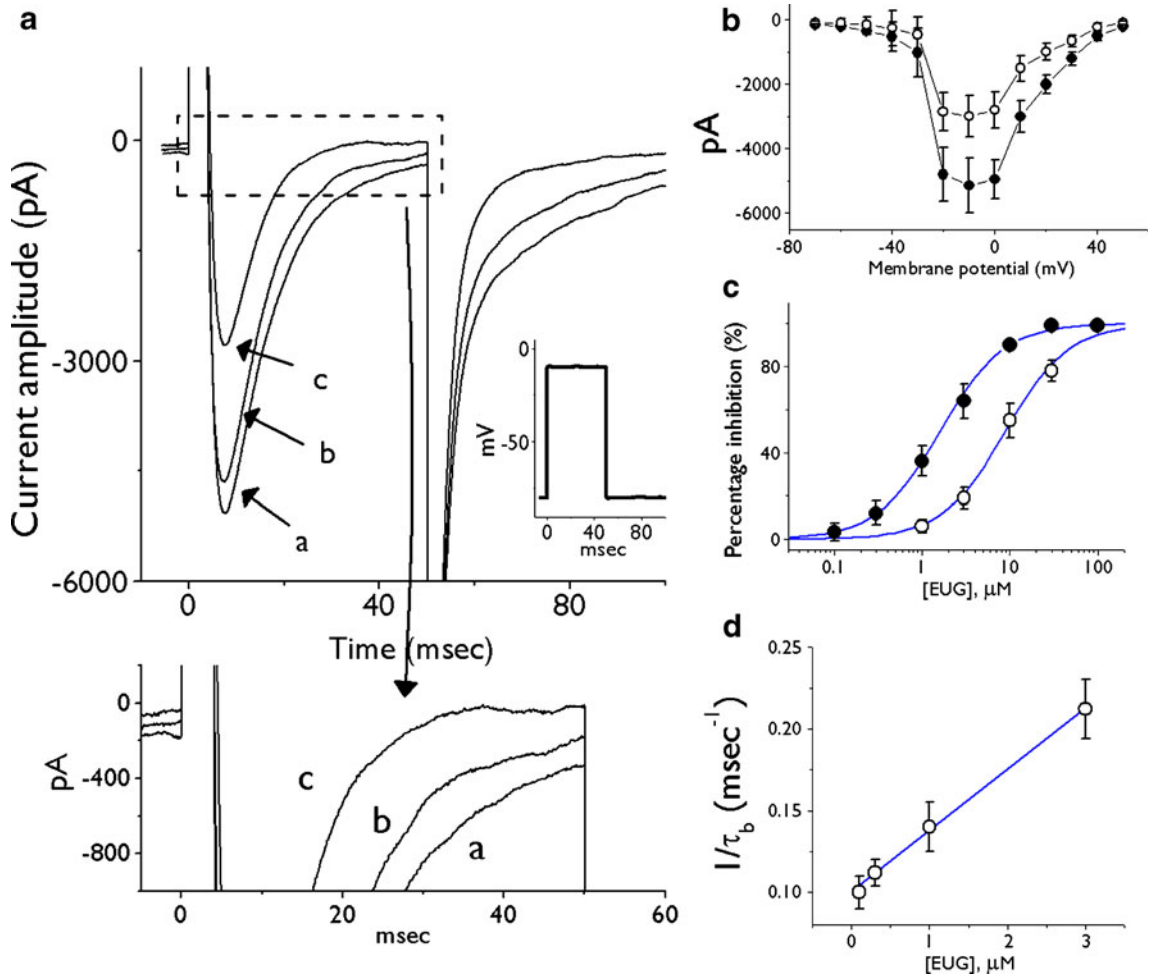

Fig. 1 Inhibitory effects of EUG on I_{Na} in differentiated NG108-15 neuronal cells. In these experiments, each pipette was loaded with a Cs^+-containing solution, and cells were bathed in Ca^{2+}-free Tyrode's solution containing 10 mM TEA. **a** Concentration-dependent inhibition of I_{Na} by EUG in an NG108-15 cell. Original current traces were obtained in the control (*a*) and during exposure to 1 μM (*b*) and 10 μM (*c*) EUG. The *lower part* in **a** indicates an expanded record from the upper part (*dashed box*), and *inset* shown in the upper part of **a** is the voltage protocol used. **b** Averaged *I-V* relationships of the transient I_{Na} obtained in control (*black circle*) and during the exposure to EUG (*white circle*). Each cell was depolarized from −80 mV to different membrane potentials with duration of 50 ms at a rate of 0.1 Hz. Each *point* represents the mean±SEM (n=6–9). **c** Concentration-response relationships for EUG-induced inhibition of I_{Na} (i.e. TTX-sensitive current) measured at the beginning (*white circle*) and end (*black circle*) of depolarizing pulses (mean±SEM, n=7–11 for each point). Smooth lines represent the best fits to the Hill equation as described in Methods. In **d**, time-dependent block of I_{Na} inactivation caused by EUG in differentiated NG108-15 neuronal cells was evaluated. The reciprocal of time constant of the rate of block ($1/\tau_b$) obtained by exponential fits of the slow component of I_{Na} inactivation ($\tau_{inact(S)}$) was plotted against the EUG concentration. Data points were well fitted by a linear regression, indicating that EUG-induced blocking occurs with a molecularity of 1. Blocking (k_{+1}) and unblocking (k_{-1}) rate constants, given by the slope and the y-axis intercept of the interpolated line, were 0.037 ms^{-1} μM^{-1} and 0.10 ms^{-1}, respectively

half-maximal concentrations (IC_{50}) required for the inhibitory effects of EUG on transient and late components of I_{Na} were 8.9 and 1.6 μM, respectively.

Therefore, it is clear that EUG significantly inhibited transient and late I_{Na} in these cells. Moreover, EUG inhibited the late component of I_{Na} more than it inhibited the transient component.

Evaluating EUG's time-dependent inhibition of I_{Na} inactivation

EUG not only showed lower I_{Na} amplitude, but also increased the degree of I_{Na} inactivation. To confirm EUG-induced inhibition of I_{Na}, we used a two-exponential process (fast and slow components) to fit the time courses of current inactivation with and without EUG treatment. EUG concentration-dependently reduced $\tau_{inact(S)}$ (Fig. 1d). However, no significant changes in the fast component of current inactivation was noted in EUG-treated cells. Therefore, increasing EUG concentration not only diminished the peak amplitude of I_{Na}, but also increased the inactivation time course of the current. Based on the first-order blocking scheme described in Methods, the relationship between $1/\tau_b$ and [B] was found to be linear with a correlation coefficient of 0.97 (Fig. 1d). The blocking (i.e. on) and unblocking (i.e. off) rate constants obtained from six to eight different cells were calculated to be 0.037 ms^{-1} μM^{-1} and 0.10 ms^{-1}, respectively. On the basis of these rate constants, the apparent dissociation constant ($K_D=k_{-1}/k_{+1}$) for the binding of EUG to Na_V channels was thus calculated to be 2.7 μM. Notably, this value is close to the estimated IC_{50} value for EUG-mediated inhibition of late I_{Na} determined from the concentration-response curve (Fig. 1c).

Effect of EUG on the $I_{Na(NI)}$ in NG108-15 neuronal cells

The $I_{Na(NI)}$ was previously demonstrated to be present in NG108-15 cells at our laboratory (Wu et al. 2009a). In a separate series of experiments, investigations were further undertaken to evaluate whether EUG has any effects on the amplitude of $I_{Na(NI)}$ in response to long-lasting ramp pulse. In these experiments, cells were bathed in Ca^{2+}-free Tyrode's solution containing 10 mM of TEA. When the cell was held at the level of −50 mV, a long-lasting ramp pulse from −100 to +50 mV was applied at a rate of 0.05 Hz. Our results showed that EUG suppressed $I_{Na(NI)}$ elicited by long ramp pulse (Fig. 2a, b). For example, cell exposure to 1 μM of EUG significantly decreased the peak amplitude of $I_{Na(NI)}$ by 50±6% from 248±32 to 123±16 pA (n=7). A subsequent application of tefluthrin (10 μM) was able to attenuate EUG-mediated inhibition of $I_{Na(NI)}$ elicited by long ramp pulse (Fig. 2c) Tefluthrin is a synthetic type-I pyrethroid known to be an activator of I_{Na} (Wu et al. 2009c). Additionally, a further application of salmeterol (10 μM), an agonist of β_2-adrenergic receptors, was not found to have any effects on EUG-induced inhibition of $I_{Na(NI)}$.

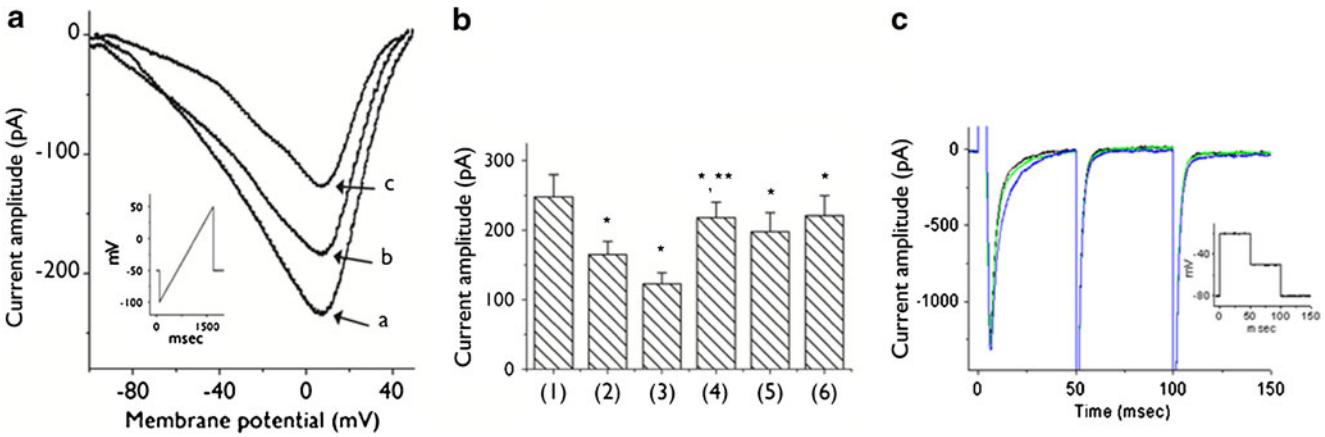

Fig. 2 Effect of EUG, eugenolol, and eugenodilol on $I_{Na(NI)}$ in differentiated NG108-15 cells. Each cell was held at −50 mV and a 1.5-s long ramp pulse from −100 to +50 mV at a rate of 0.05 Hz was applied. In **a,** original current traces in response to ramp pulse were obtained in the absence (*a*) and presence of 0.3 μM (*b*) and 1 μM (*c*) EUG. The *inset* shown in **a** indicates the voltage protocol used. In **b**, the *bar graph* shows a summary of data depicting the effect of EUG, tefluthrin, eugenolol, and eugenodilol. *(1)*: control; *(2)*: 0.3 μM EUG; *(3)* 1 μM EUG; *(4)* 1 μM EUG plus 10 μM tefluthrin; *(5)* eugenolol (10 μM); *(6)* eugenodilol (10 μM). In EUG plus tefluthrin experiments, tefluthrin (10 μM) was subsequently applied 2 min after addition of EUG (1 μM). Each *bar* indicates the mean±SEM of data from six to nine cells. *Single asterisk*: significantly different from control. *Double asterisk*: significantly different from EUG (0.3 μM) alone group. In **c**, the effect of EUG on tefluthrin-induced change in I_{Na} inactivation kinetics in NG108-15 neuronal cells. Cells were bathed in Ca^{2+}-free Tyrode's solution containing 10 mM tetraethylammonium chloride. The recording pipette was filled with a Cs^+-containing solution. *Inset* indicates the voltage protocol used. *Black*: control; *blue*: in the presence of tefluthrin (10 mM); *green*: in the presence of tefluthrin plus EUG (1 μM). Notably, EUG can reverse tefluthrin-induced slowing in the inactivation time course of I_{Na}

Effect of EUG and tetrandrine on $I_{Ca,L}$ in NG108-15 neuronal cells

Previous work has showed the ability of EUG to decrease the amplitude of voltage-gated Ca^{2+} currents in heart cells, in isolated aortae, and in the E52 cell line (Sensch et al. 2000; Damiani et al. 2003, 2004; Chung et al. 2008). We also tested whether EUG has any effects on $I_{Ca,L}$ in differentiated NG108-15 cells. As shown in Fig. 3, when the cell was depolarized from −50 to 0 mV with a duration of 300 ms, the peak amplitude of $I_{Ca,L}$ was not found to differ significantly between the absence and presence of 3 μM EUG. However, EUG at a concentration of 10 μM significantly diminished $I_{Ca,L}$ by about 20%. Neither activation nor inactivation time course of $I_{Ca,L}$ was affected in the presence of 10 μM EUG. Moreover, tetrandrine (3 μM), a bisbenzyltetrahydroisoquinoline alkaloid known to be a blocker of $I_{Ca,L}$ (Wu et al. 1998), was effective in reducing the peak amplitude of $I_{Ca,L}$ in these cells. Thus, it shows that EUG at the concentrations less than 3 μM does not significantly alter the magnitude of $I_{Ca,L}$. As compared with I_{Na} or $I_{Na(NI)}$, $I_{Ca,L}$ present in NG108-15 cells is relatively unresponsive to inhibition by EUG.

Inhibitory effect of EUG on $I_{K(DR)}$ in NG108-15 cells

A previous study demonstrated that EUG exerts inhibitory effects on K^+ outward currents in heart cells (Sensch et al. 2000). We next evaluated whether this agent has any effects on $I_{K(DR)}$ in these neuronal cells. To record $I_{K(DR)}$, cells were bathed in Ca^{2+}-free Tyrode's solution containing TTX (1 μM) and $CdCl_2$ (0.5 mM). As shown in Fig. 4, when the cell was held at −50 mV and the depolarizing pulses from −60 to +30 mV in 10-mV increments were applied, a family of K^+ outward-rectifying currents with little or no inactivation was elicited (Wu et al. 2001). Within 2 min of exposing the cell to EUG (10 μM), the amplitude of $I_{K(DR)}$ measured at the end of 300-ms depolarizing pulses was progressively reduced (Fig. 4). For example, when $I_{K(DR)}$ was elicited by depolarizing pulses from −50 to +30 mV, application of 10 μM EUG significantly diminished the amplitude of $I_{K(DR)}$ by 24±2% from 1088±98 to 831±85 pA (n=11). When the duration of depolarizing pulses was prolonged to 1 s, applying 10 μM EUG had little or no modifications on $I_{K(DR)}$ inactivation. Additionally, applying 3 μM EUG did not significantly diminish the amplitude of $I_{K(DR)}$ (data not shown). Therefore, unlike I_{Na}, $I_{K(DR)}$ present in NG108-15 cells tends to be relatively refractory to inhibition by EUG.

Effects of EUG on spontaneous APs in differentiated NG108-15 neuronal cells

The effect of EUG on repetitive firing of APs was investigated in these cells. Cells were bathed in normal Tyrode's solution containing 1.8 mM of $CaCl_2$, and current-clamp recordings were performed with a K^+-containing pipette solution. The typical effect of EUG on spontaneous APs in

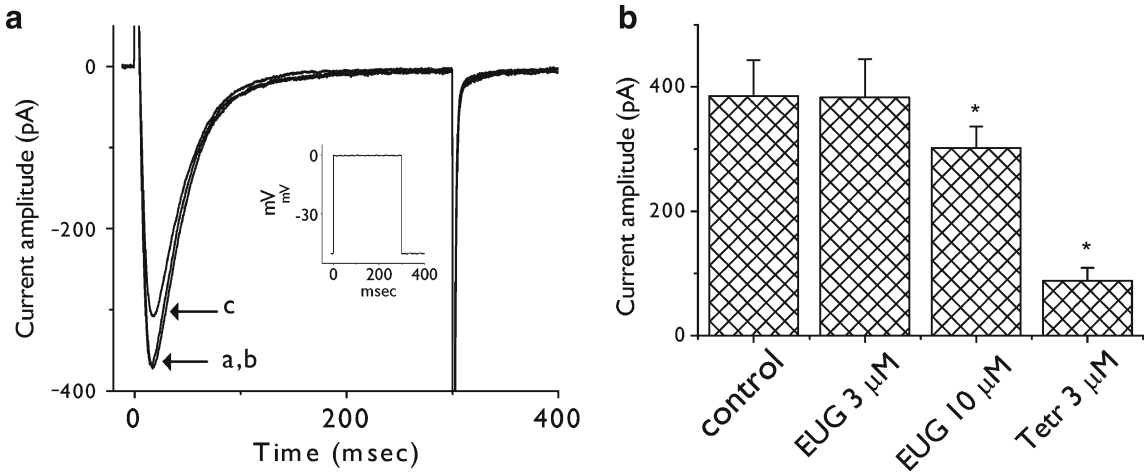

Fig. 3 Effect of EUG and tetrandrine on $I_{Ca,L}$ in differentiated NG108-15 cells. Cells were bathed in normal Tyrode's solution containing 1.8 mM $CaCl_2$ and 10 mM TEA. The recording pipette was filled with a Cs^+-containing solution. **a** Current traces of $I_{Ca,L}$ evoked by the depolarizing pulse from a holding potential of −50 to 0 mV. Trace a is control, and traces b and c are $I_{Ca,L}$ recorded 2 min after application of 3 and 10 μM EUG, respectively. The *inset* in **a** indicates the voltage protocol used. **b** Summary of data depicting the effects of EUG and tetrandrine (Tetr) on the peak amplitude of $I_{Ca,L}$. Each *bar* indicates the mean±SEM of data from 7 to 12 cells. *Single asterisk*: significantly different from control

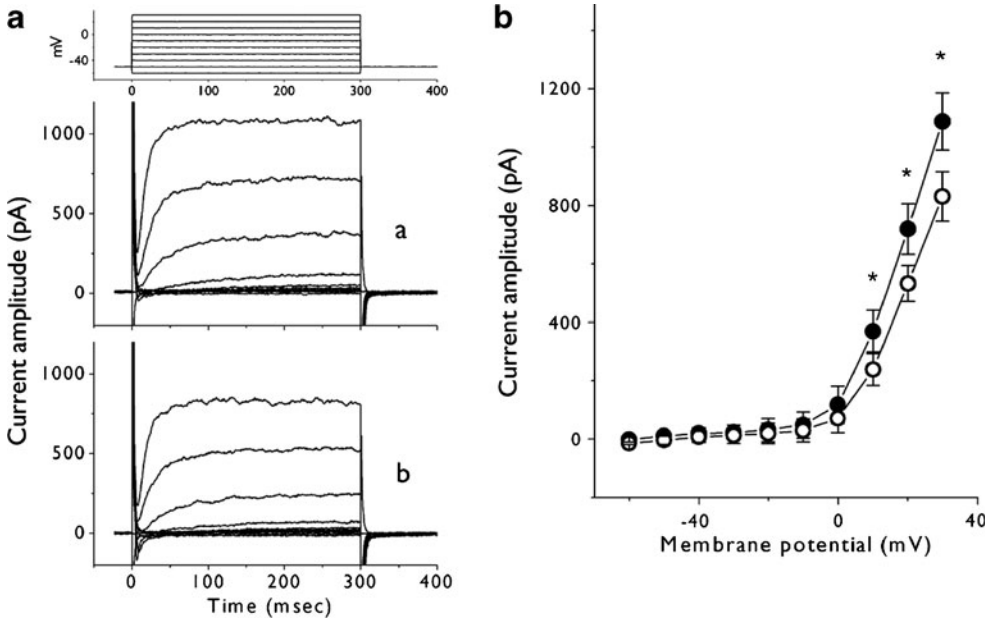

Fig. 4 Effect of EUG on $I_{K(DR)}$ in differentiated NG108-15 cells. Cells were bathed in Ca^{2+}-free Tyrode's solution containing 1 μM TTX and 0.5 mM $CdCl_2$. **a** Superimposed current traces obtained in the absence (*a*) and presence (*b*) of 10 μM EUG. The *upper part* of **a** indicates the voltage protocol examined. Note that neither activation nor inactivation time course of $I_{K(DR)}$ can be altered in the presence of EUG. **b** *I–V* relationships of $I_{K(DR)}$ in the absence (*black circle*) and presence (*white circle*) of 10 μM EUG. Each cell was depolarized from −50 mV to various potentials ranging from −60 to +30 mV at a rate of 0.1 Hz. Current amplitudes were measured at the end of depolarizing pulses. Each point indicates the mean±SEM of data from 9 to 12 cells. *Single asterisk*: significantly different from controls

these cells is illustrated in Fig. 5a. When cells were exposed to EUG, the repetitive firing of APs was robustly diminished (Fig. 5b). For example, EUG (1 μM) significantly reduced the firing frequency of APs to 1.68±0.08 Hz (n=7) by 26±3% from a control value of 2.27±0.14 Hz (n=7). The firing of spontaneous APs was almost returned to the control value

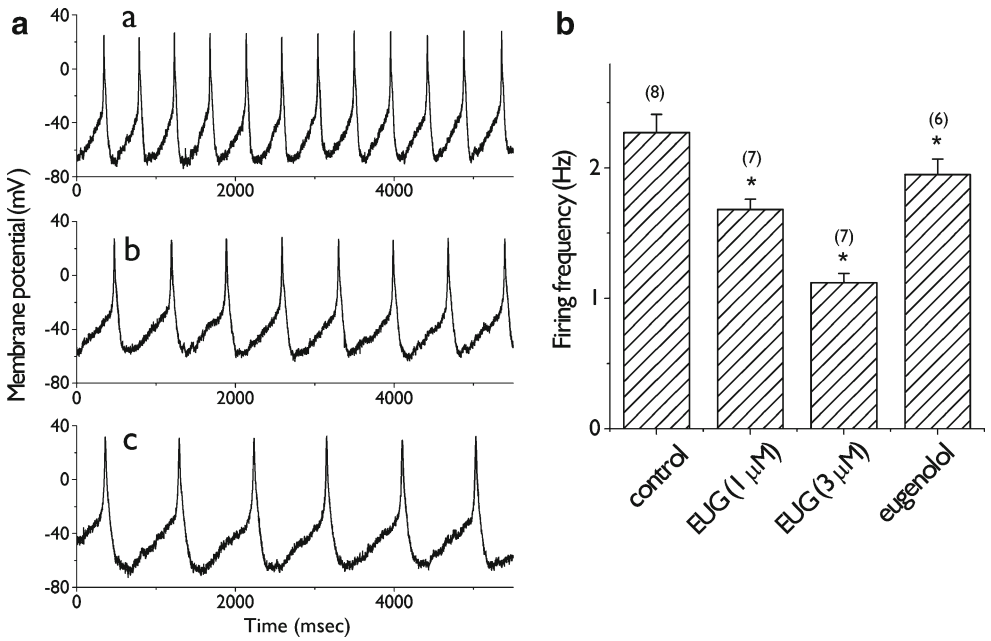

Fig. 5 Effect of EUG and eugenolol on spontaneous APs in NG108-15 cells. Cells were bathed in normal Tyrode's solution containing 1.8 mM $CaCl_2$. The experiments were performed under current-clamp conditions. **a** Original traces obtained in the control (*a*) and during the exposure to 1 μM (*b*) and 3 μM (*c*) EUG. **b** *Bar graph* showing the effect of EUG and eugenolol (10 μM) on firing frequency of APs. The *parentheses* shown in each bar are the number of cells examined. Values are the mean±SEM. *Single asterisk*: significantly different from control

after washout of EUG. However, eugenolol (10 μM) only slightly decreased the firing frequency by around 14 %. Therefore, it is clear that EUG can regulate the firing of neuronal APs. The decrease in the firing frequency of APs caused by EUG at concentrations less than 10 μM can be primarily explained by its depressant actions on I_{Na} and $I_{Na(NI)}$ in NG108-15 neuronal cells.

Effects of EUG on repetitive firing of action potentials in modeled neurons

In order to predict how EUG alters the discharge pattern of hippocampal neurons, a modified Pinsky and Rinzel simulation modeling was implemented (Huang et al. 2008). Figure 6 illustrates the time course of repetitive firing of action potentials and corresponding changes in I_{Na} and $I_{Na(NI)}$ from a modeled neuron. In the control, the firing frequency is 2.7 Hz. When the maximal conductances of I_{Na} and $I_{Na(NI)}$ were arbitrarily reduced to 17.1 and 0.3 nS from control values of 18 and 0.5 nS, respectively, the discharge rate was declined to 1.8 Hz. This result resembled our experimental observations showing that application of EUG (1 μM) reduced the firing frequency by approximately 28% (Fig. 5).

The effects of EUG on pilocarpine-induced acute seizures

The EUG group showed a similar latency to the first seizure (stage 1; mean±SEM, 28±2.2 min) with the control group (25±2.3 min) , the RLZ+EUG group (26±2.6 min), the eugenolol group (24.5±1.5 min) and the eugenodilol group (26.9±2.5 min). Nevertheless, in terms of the seizure severity, the percentage of severe seizures (stages 3, 4 and 5) in the EUG group was significantly less than that in the other four groups (EUG, 25% (5/20); control, 70% (14/20); RLZ+EUG, 55% (11/20); eugenolol, 60% (12/20); eugenodilol, 65% (13/20; $p<0.05$). For acute status epilepticus-related mortality, it was significantly lower in the EUG group (15%; 3/20), than it is in the control group (40%; 8/20), the RLZ+EUG group (30%; 6/20), the Eugenolol (30%; 6/20) and the eugenodilol (35%; 7/20) ($p<0.05$; Fig. 7).

Discussion

The major findings of this study are as follows: First, in differentiated NG108-15 neuronal cells, EUG differentially inhibited the transient and late components of I_{Na} in a concentration-dependent manner. Second, EUG was able

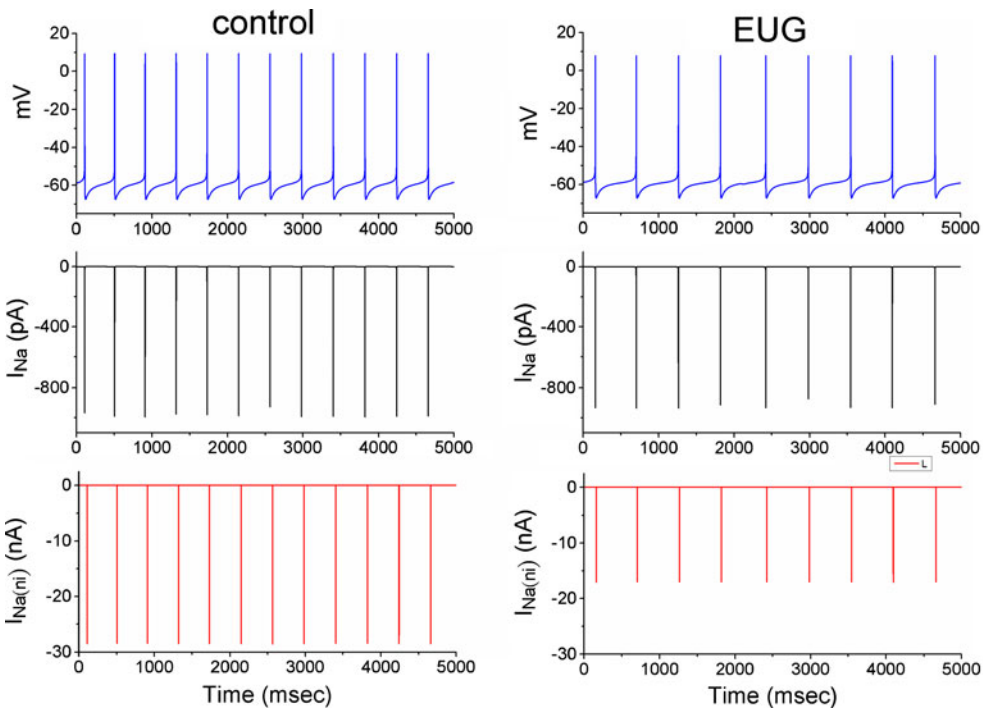

Fig. 6 Simulation modeling used to mimic EUG effects on the firing of action potentials (APs, *upper*, *blue color*), I_{Na} (*middle*, *black color*) and $I_{Na(NI)}$ (*lower*, *red color*) in NG108-15 neurons. The model was based on the model of Huang et al. (2008) in which the non-inactivating component of I_{Na} ($I_{Na(NI)}$) was incorporated. The formulation of $I_{Na(NI)}$ was described in Methods. To mimic the effect of EUG (1 μM) on electrical behavior of NG108-15 cells, the I_{Na} conductance (g_{Na}) was reduced from 18 to 17.1 nS and the $I_{Na(NI)}$ conductance ($g_{Na(NI)}$) was reduced from 0.5 to 0.3 nS

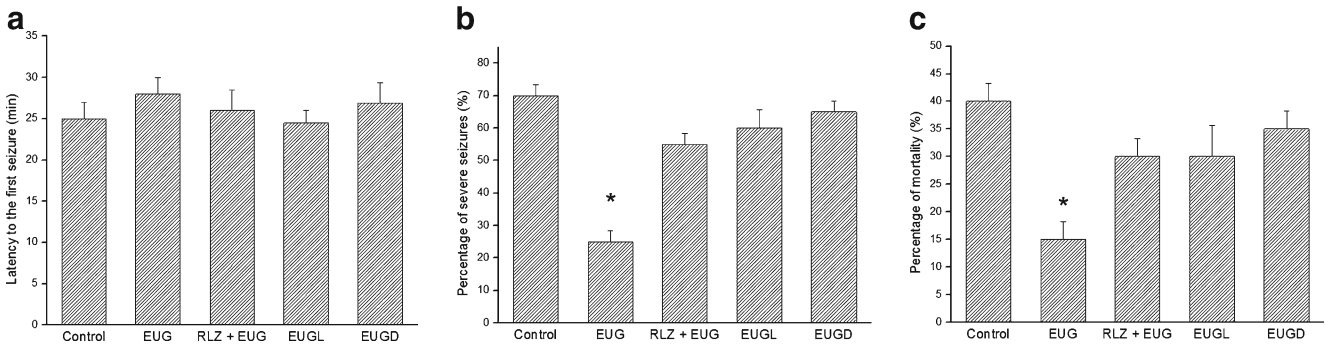

Fig. 7 Pilocarpine-induced acute seizures in the control, EUG, RLZ+ EUG, eugenolol and eugenodilol groups. **a** Similar latency to the first seizure (stage 1) in the five groups (p=0.35). **b** The EUG group had significantly lower percentage of severe seizures (stage 3–5; *p= 0.041). **c**: The EUG group had lower status epilepticus-related mortality in the acute period (*p=0.02; n =20 in each group) *Single asterisk*: significantly different from control, *RLZ+ EUG*, *EUGL* and *EUGD* group. *EUGL* eugenolol, *EUGD* eugenodilol

to diminish the amplitude of $I_{Na(NI)}$ evoked by long-lasting ramp pulse, and tefluthrin reversed the EUG-induced inhibition of $I_{Na(NI)}$. Third, at a high concentration, EUG could reduce the amplitude of $I_{Ca,L}$ and $I_{K(DR)}$. Fourth, EUG could decrease the firing frequency of spontaneous APs. Fifth, from simulation modeling, we verified clearly that EUG can effectively decrease the firing frequency by attenuating I_{Na} and $I_{Na(NI)}$, thereby leading to a reduction of neuronal excitability. Lastly, EUG ameliorated pilocarpine-induced seizures in SD rats and the effects could be occluded by riluzole, an $I_{Na(NI)}$ anatagonist.

A notable feature of the block of I_{Na} caused by EUG in these cells is that the initial rising phase of the current (i.e. the activation time course) was unaffected. It is thus likely that before channel activation, there should be the absence of any significant resting block of Na_V channels. Moreover, no discernible change in the I–V relationship of the transient I_{Na} was found in the presence of EUG. However, another important finding in this study is that the inhibitory effects of EUG on I_{Na} are not limited to its inhibition of the peak amplitude of this current. In other words, increasing the EUG concentration not only reduced the peak current of I_{Na}, but also accelerated the apparent inactivation. The EUG molecule appears to the blocking site only when the channel is in the open state. This feature can be incorporated in a minimal binding scheme (i.e. closed ↔ open ↔ open-blocked (Wu et al. 2009b). Therefore, the EUG-mediated block of I_{Na} can be interpreted as suggesting that it preferentially binds to and blocks an open state of the Na_V channel.

We clearly demonstrated that EUG in the concentration range of 0.1-1 μM had almost no effect on the transient component of I_{Na}; however, it indeed effectively blocked the late component of I_{Na}. The IC_{50} values of EUG required for the inhibition of the transient and late I_{Na} tend to be lower than those for its inhibitory effect on $I_{Ca,L}$ or $I_{K(DR)}$. Therefore, the experimental results presented herein indicate that there is a selective block of late I_{Na} by EUG. The reduction of AP firing caused by EUG at concentrations less than 10 μM could be primarily explained by its ability to inhibit the transient and late components of I_{Na} in NG108-15 neuronal cells, partly because $I_{Ca,L}$ was relatively not subject to block by EUG.

EUG and its newly designed compounds (e.g. eugenolol and eugenodilol) have been previously demonstrated to exhibit the antagonistic activity of β-adrenergic receptors (Chen et al. 1997; Huang et al. 1999; Wu et al. 2000). However, EUG-induced inhibition of $I_{Na(NI)}$ presented herein was found to be attenuated by a further application of tefluthrin, but not by salmeterol, an agonist of β_2-adrenergic receptors. This suggests that the inhibition of I_{Na} and $I_{Na(NI)}$ caused by EUG is direct and appears to be not necessarily associated with the binding to β-adrenergic receptors, although the binding to β_2-adrenergic receptors is reported to stimulate γ-secretase and accelerate β-amyloid plaque formation in brain (Ni et al. 2006). Additionally, neither eugenolol nor eugenodilol at concentrations less than 1 μM could produce an inhibitory effect on I_{Na} or $I_{Na(NI)}$ present in these cells. It is thus tempting to speculate that a chemical modification in the 4-hydroxy group of EUG diminishes its inhibitory effects on Na_V channels, although it is able to enhance the antagonistic activities of β-adrenergic receptors (Wu et al. 2000).

EUG has been found to have anticonvulsant effect (Dallmeier and Carlini 1981; Sayyah et al. 2002). It also protects neurons from excitotoxic and oxidative injury (Wie et al. 1997). As enhancement of $I_{Na(NI)}$ may be a common underlying mechanism in some forms of epilepsy (Lossin et al. 2002; Segal 2002; Chen et al. 2011), the inhibitory effect on $I_{Na(NI)}$ of EUG, as shown in our study, potentially supports the role of EUG in treating some epileptic disorders. Additionally, as an anticonvulsant agent with a primary effect on sodium channels, it could reduce synaptic transmission without significantly interfering neuronal synaptic plasticity (Ardjmand et al. 2006). Moreover, it is noted that the IC_{50} value required for EUG-induced inhibition of I_{Na} in

this study is about 1 μM. A recent report (Lionnet et al. 2010) showed that there was a high ratio of brain-to-plasma and spinal cord-to-plasma, suggesting that EUG can penetrate the brain well. The anti-epileptic effect of EUG observed in this study may occur at a concentration achievable in humans. Therefore, it is anticipated that there would be a link between antiepileptic activity and its inhibitory action on I_{Na}. Nevertheless, further studies are needed to determine the extent to which EUG-mediated inhibition of I_{Na} contribute to its management of epileptic attacks.

Riluzole, a neuronal excitability-modulator with neuroprotective properties, is a specific antagonist of persistent sodium current but not fast sodium current in mammalian central neurons (Urbani and Belluzzi 2000; Mathew et al. 2010). Our study showed that the EUG's effect on $I_{Na(NI)}$ was occluded by pretreated RLZ, compared to EUG alone. This basically supported the notion that the anticonvulsant effect of EUG, at least partially, derived from effect on $I_{Na(NI)}$. We found that the group EUG+RLZ did not have strong anticonvulsant effect (though relatively smaller percentage of severe seizures) and did not have a distinct effect on seizure latency. There exist some controversies regarding riluzole's effects on neuronal excitability. A report showed that riluzole might lower the level of pilocarpine in both brain and plasma, thereby altering its effect on pilocarpine-induced seizure activity (Zgrajka et al. 2010); nevertheless, one study reported riluzole's paradoxical effect on worsening neuronal excitability (Peña and Tapia 2000). Further pharmacokinetic and mechanistic studies in epileptic animals regarding riluzole and EUG would be required.

Expression of $Na_V1.7$ and $Na_V1.8$ has been shown to be up-regulated in dorsal root ganglion neurons during long-lasting inflammatory reaction with carrageenan injection (Black et al. 2004). The inhibition of Na_V channels (e.g. $Na_V1.7$ and $Na_V1.8$) expressed in the sensory nerve terminals in the teeth (Djouhri et al. 2003; Warren et al. 2008) might be the molecular basis for the actions of EUG in treating pain. Although the distribution and level of expression of Na_V channels in chronic epileptic circuits (e.g. $Na_V1.7$ and $Na_V1.8$) remains to be investigated, the potential for selective blockade of late I_{Na} and $I_{Na(NI)}$ may have important clinical implications in treating some neuronal hyperexcitability disorders.

In conclusion, these results led us to suggest that the pain-relieving and seizure-ameliorating effect of EUG may be primarily associated with its propensity to interact with Na_V channels. By synergistic inhibition of I_{Na} and $I_{Na(NI)}$, EUG can be a potential pharmacological tool used in characterization of the properties of Na_V channels and in clinical medicine such as ameliorating epileptic seizures.

Acknowledgements This research project was funded by the National Science Council (NSC-98-2320-B-006-027-MY3 and NSC-98-2314-B-006-042-MY2) and the Program for Promoting Academic Excellence and Developing World Class Research Centers, Ministry of Education, Taiwan. This work was also supported in part by a grant from Buddhist Dalin Tzu-Chi General Hospital (DTCRD98-08), Chiayi County, Taiwan. The authors are grateful to Dr. Dong Chun Wu (Department of Neurology, University of British Columbia, Canada) for his critical comments on the manuscript.

Conflicts of interest None of the authors in this study have any potential conflict of interest or financial interests to disclose.

References

Ardjmand A, Fathollahi Y, Sayyah M, Kamalinejad M, Omrani A (2006) Eugenol depresses synaptic transmission but does not prevent the induction of long-term potentiation in the CA1 region of rat hippocampal slices. Phytomedicine 13:146–151

Benarroch EE (2010) Neuronal voltage-gated calcium channels: brief overview of their function and clinical implications in neurology. Neurology 74:1310–1315

Bender IB (2000) Pupal pain diagnosis—a review. J Endod 26:175–179

Black JA, Liu S, Tanaka M, Cummins TR, Waxman SG (2004) Changes in the expression of tetrodotoxin-sensitive sodium channels within dorsal root ganglia neurons in inflammatory pain. Pain 108:237–247

Chen SJ, Huang YC, Wu BN, Chen IJ (1997) Eugenolol: an eugenol-derived β-adrenoceptor blocker with partial β_2-agonist and calcium mobilization inhibition associated vasorelaxant activities. Drug Dev Res 40:239–250

Chen BS, Peng H, Wu SN (2009) Dexmedetomidine, an α_2-adrenergic agonist, inhibits neuronal delayed-rectifier potassium current and sodium current. Br J Anaesth 103:244–254

Chen S, Su H, Yue C, Remy S, Royeck M, Sochivco D, Opitz T, Beck H, Yaari Y (2011) An increase in persistent sodium current contributes to intrinsic neuronal bursting after status epilepticus. J Neurophysiol 105:117–129

Cho JS, Kin TH, Lim JM, Song JH (2008) Effects of eugenol on Na^+ currents in rat dorsal root ganglion neurons. Brain Res 1243:53–62

Chung G, Rhee JN, Jung SJ, Kim JS, Oh SB (2008) Modulation of $Ca_V2.3$ calcium channel currents by eugenol. J Dent Res 87:137–141

Cifelli P, Grace AA (2011) Pilocarpine-induced temporal lobe epilepsy in the rat is associated with increased dopamine neuron activity. Int J Neuropsychopharmacol 12:1–8

Coetzee WA, Amarillo Y, Chiu J, Chow A, Lau D, McCormack T, Moreno H, Nadal MS, Ozaita A, Pountney D, Saganich M, Vega-Saenz de Miera E, Rudy B (1999) Molecular diversity of K^+ channels. Ann N Y Acad Sci 868:233–285

Dallmeier K, Carlini EA (1981) Anesthetic, hypothermic, myorelaxant and anticonvulsant effects of synthetic eugenol derivatives and natural analogues. Pharmacology 22:113–127

Dallmeier K, Zelger JL, Carlini EA (1983) New anticonvulsants derived from 4-allyl-2-methoxyphenol (Eugenol): comparison with common antiepileptics in mice. Pharmacology 27:40–49

Damiani CE, Rossoni LV, Vassallo DV (2003) Vasorelaxant effects of eugenol on rat thoracic aorta. Vascul Pharmacol 40:59–66

Damiani CE, Moreira CM, Zhang HT, Creazzo TL, Vassallo DV (2004) Effects of eugenol, an essential oil, on the mechanical and electrical activities of cardiac muscle. J Cardiovasc Pharmacol 44:688–695

Djouhri L, Newton R, Levinson SR, Berry CM, Carruthers B, Lawson SN (2003) Sensory and electrophysiological properties of guinea-

pig sensory neurones expressing $Na_V1.7$ (PN_1) Na^+ channel a subunit protein. J Physiol 546:565–576

Duarte FS, Gavioli EC, Duzzioni M, Hoeller AA, Canteras NS, De Lima TC (2010) Short- and long-term anxiogenic effects induced by a single injection of subconvulsant doses of pilocarpine in rats: investigation of the putative role of hippocampal pathways. Psychopharmacology (Berl) 212:653–661

Earl DE, Tietz EI (2011) Inhibition of recombinant L-type voltage-gated calcium channels by positive allosteric modulators of GABAA receptors. J Pharmacol Exp Ther 337:301–311

Freire CM, Marques MO, Costa M (2006) Effects of seasonal variation on the central nervous system activity of *Ocimum gratissimum* L. essential oil. J Ethnopharmacol 105:161–166

He YL, Zhan XQ, Yang G, Sun J, Mei YA (2010) Amoxapine inhibits the delayed rectifier outward K+current in mouse cortical neurons via cAMP/protein kinase A pathways. J Pharmacol Exp Ther 332:437–445

Huang YC, Wu BN, Lin YT, Chen SJ, Chiu CC, Cheng CJ, Chen IJ (1999) Eugenodilol: a third-generation β-adrenoceptor blocker, derived from eugenol, with α-adrenoceptor blocking and β_2-adrenoceptor agonist-associated vasorelaxant activities. J Cardiovasc Pharmacol 34:10–20

Huang CW, Huang CC, Lin MW, Tsai JJ, Wu SN (2008) The synergistic inhibitory actions of oxcarbazepine on voltage-gated sodium and potassium currents in differentiated NG108-15 neuronal cells and model neurons. Int J Neuropsychopharmacol 11:597–610

Huang CW, Cheng JT, Tsai JJ, Wu SN, Huang CC (2009) Diabetic hyperglycemia aggravates seizures and status epilepticus-induced hippocampal damage. Neurotox Res 15:71–81

Huang CW, Wu SN, Cheng JT, Tsai JJ, Huang CC (2010) Diazoxide reduces status epilepticus neuron damage in diabetes. Neurotox Res 17:305–316

Huang CW, Wu YJ, Wu SN (2011) Modification of activation kinetics of delayed rectifier K+currents and neuronal excitability by methyl-β-cyclodextrin. Neuroscience 176:431–441

Irie Y, Keung WM (2003) *Rhizoma acori graminei* and its active principles protect PC-12 cells from the toxic effect of amyloid-β peptide. Brain Res 963:282–289

Kawaguchi A, Asano H, Matsushima K, Wada T, Yoshida S, Ichida S (2007) Enhancement of sodium current in NG108-15 cells during neural differentiation is mainly due to an increase in $Na_V1.7$ expression. Neurochem Res 32:1469–1475

Köseoğlu BG, Tanrikulu S, Sübay RK, Sencer S (2006) Anesthesia following overfilling of a root canal sealer into the mandibular canal: a case report. Oral Surg Oral Med Oral Pathol Oral Radiol Endod 101:803–806

Lin MW, Yang SR, Huang MH, Wu SN (2004) Stimulatory actions of caffeic acid phenethyl ester, a known inhibitor of NF-kappaB activation, on Ca^{2+}-activated K^+ current in pituitary GH3 cells. J Biol Chem 279:26885–26892

Lin MW, Wang YJ, Liu SI, Lin AA, Lo YC, Wu SN (2008) Characterization of aconitine-induced block of delayed rectifier K^+ current in differentiated NG108-15 neuronal cells. Neuropharmacology 54:912–923

Lionnet L, Beaudry F, Vachon P (2010) Intrathecal eugenol administration alleviates neuropathic pain in male Sprague–Dawley rats. Phytother Res 24:1645–1653

Lossin C, Wang DW, Rhodes TH, Vanoye CG, George AL (2002) Molecular basis of an inherited epilepsy. Neuron 34:877–884

Mathew SJ, Murrough JW, aan het Rot M, Collins KA, Reich DL, Charney DS (2010) Riluzole for relapse prevention following intravenous ketamine in treatment-resistant depression: a pilot randomized, placebo-controlled continuation trial. Int J Neuropsychopharmacol 13:71–82

Meves H, Schwarz JR, Wulfsen I (1999) Separation of M-like current and ERG current in NG108-15 cells. Br J Pharmacol 127:1213–1223

Müller M, Pape HC, Speckmann EJ, Gorji A (2006) Effect of eugenol on spreading depression and epileptiform discharges in rat neocortical and hippocampal tissues. Neuroscience 140:743–751

Ni Y, Zhao X, Bao G, Zou L, Teng L, Wang Z, Song M, Xiong J, Bai Y, Pei G (2006) Activation of β_2-adrenergic receptor stimulates γ-secretase activity and accelerates amyloid plaque formation. Nat Med 12:1390–1396

Ohkubo T, Kitamura K (1997) Eugenol activates Ca^{2+}-permeable currents in rat dorsal root ganglion cells. J Dent Res 76:1737–1744

Park CK, Kim K, Jung SJ, Kim MJ, Ahn DK, Hong SD, Kim JS, Oh SB (2009) Molecular mechanism for local anesthetic action of eugenol in the rat trigeminal system. Pain 144:84–94

Peña F, Tapia R (2000) Seizures and neurodegeneration induced by 4-aminopyridine in rat hippocampus in vivo: role of glutamate- and GABA-mediated neurotransmission and of ion channels. Neuroscience 101:547–561

Pinsky PF, Rinzel J (1994) Intrinsic and network rhythmogenesis in a reduced Traub model for CA3 neurons. J Comput Neurosci 1:39–60

Pitkanen A, Schwartzkroin PA, Moshe SL (2006) Models of seizures and epilepsy. Elsevier Academic Press, Burlington

Pourgholami MH, Kamalinejad M, Javadi M, Majzoob S, Sayyah M (1999) Evaluation of the anticonvulsant activity of the essential oil of Eugenia caryophyllata in male mice. J Ethnopharmacol 64:167–171

Racine RJ, Burnham WM, Gartner JG, Levitan D (1973) Rates of motor seizure development in rats subjected to electrical brain stimulation: strain and inter-stimulation interval effects. Electroencephalogr Clin Neurophysiol 35:553–556

Sayyah M, Valizadeh J, Kamalinejad M (2002) Anticonvulsant activity of the leaf essential oil of Laurus nobilis against pentylenetetrazole- and maximal electroshock-induced seizures. Phytomedicine 9:212–216

Segal MM (2002) Sodium channels and epilepsy electrophysiology. Novartis Found Symp 241:173–180

Segal MM, Douglas AF (1997) Late sodium channel openings underlying epileptiform activity are preferentially diminished by the anticonvulsant phenytoin. J Neurophysiol 77:3021–3034

Sensch O, Vierling W, Brandt W, Reiter M (2000) Effects of inhibition of calcium and potassium currents in guinea-pig cardiac contraction: comparison of β-caryophyllene oxide, eugenol, and nifedpine. Br J Pharmacol 131:1089–1096

Stafstrom CE (2007) Persistent sodium current and its role in epilepsy. Epilepsy Curr 7:15–22

Tsai TY, Tsai YC, Wu SN, Liu YC (2006) Tramadol-induced blockade of delayed rectifier potassium current in NG108-15 neuronal cells. Eur J Pain 10:597–601

Urbani A, Belluzzi O (2000) Riluzole inhibits the persistent sodium current in mammalian CNS neurons. Eur J Neurosci 12:3567–3574

Warren CA, Mok L, Gondon S, Fouad AF, Gold MS (2008) Quantification of neural protein in extirpated tooth pulp. J Endod 34:7–10

Wie MB, Won MH, Lee KH, Shin JH, Lee JC, Suh HW, Song DK, Kim YH (1997) Eugenol protects neuronal cells from excitotoxic and oxidative injury in primary cortical cultures. Neurosci Lett 225:93–96

Won MH, Lee JC, Kim YH, Song DK, Suh HW, Oh YS, Kim JH, Shin TK, Lee YJ, Wie MB (1998) Postischemic hypothermia induced by eugenol protects hippocampal neurons from global ischemia gerbils. Neurosci Lett 254:101–104

Wu SN, Li HF, Jan CR (1998) Regulation of Ca^{2+}-activated nonselective cationic currents in rat pituitary GH_3 cells: involvement in L-type Ca^{2+} current. Brain Res 812:133–141

Wu BN, Shen KP, Lin RJ, Huang YC, Chiang LC, Lo YC, Lin CY, Chen IJ (2000) Lipid solubility of vasodilatory vanilloid-type β-

blockers on the functional and binding activities of β-adrenoceptor subtypes. Gen Pharmacol 34:321–328

Wu SN, Lo YK, Chen H, Li HF, Chiang HT (2001) Rutaecarpine-induced block of delayed rectifier K^+ current in NG108-15 neuronal cells. Neuropharmacology 41:834–843

Wu SN, Chen BS, Hsu TI, Peng H, Wu YH, Lo YC (2009a) Analytical studies of rapidly inactivating and noninactivating sodium currents in differentiated NG108-15 neuronal cells. J Theor Biol 259:828–836

Wu SN, Chen BS, Wu YH, Peng H, Chen LT (2009b) The mechanism of the actions of oxaliplatin on ion currents and action potentials in differentiated NG108-15 neuronal cells. Neurotoxicology 30:677–685

Wu SN, Wu YH, Chen BS, Lo YC, Liu YC (2009c) Underlying mechanism of actions of tefluthrin, a pyrethroid insecticide, on voltage-gated ion currents and on action currents in pituitary tumor (GH_3) cells and GnRH-secreting (GT1-7) neurons. Toxicology 258:70–77

Yang BH, Piao ZG, Kim YB, Lee CH, Lee JK, Park K, Kim JS, Oh SB (2003) Activation of vanilloid receptor 1 (VR1) by eugenol. J Dent Res 82:781–785

Zgrajka W, Nieoczym D, Czuczwar M, Kiś J, Brzana W, Wlaź P, Turski WA (2010) Evidences for pharmacokinetic interaction of riluzole and topiramate with pilocarpine in pilocarpine-induced seizures in rats. Epilepsy Res 88:269–274